Variations of the relative palaeointensity of the geomagnetic field in western Europe in the interval 25-10 kyr BP as deduced from analyses of lake sediments

Nicolas Thouveny

Geophys. J. R. astr. Soc. (1987) **91**, 123–142

Variations of the relative palaeointensity of the geomagnetic field in western Europe in the interval 25–10 kyr BP as deduced from analyses of lake sediments

N. Thouveny *Laboratoire de Géologie du Quaternaire, CNRS, Luminy, Case 907, 13288 Marseille cedex 9, France*

Accepted 1987 March 24. Received 1987 March 24; in original form 1986 October 20

Summary. Two independent methods have been applied on late glacial and glacial homogeneous lacustrine sediments in order to obtain an evaluation of the geomagnetic field palaeointensity in the interval 10 000–25 000 yr BP. The anhysteretic remanent magnetization (ARM) normalization method and the stirred remanent magnetization (StRM) normalization method yield relative palaeointensity curves which can be critically compared. The StRM normalization curve, considered as the most reliable, shows successive oscillations with periods ranging from 1500 to 11 000 yr. The lowest values of the field intensity occur at 10 000 and 21 000 yr BP and the highest value occurs at 15 000 yr BP.

Key words: glacial lacustrine sediments, anhysteretic remanent magnetization, stirred remanent magnetization, geomagnetic field palaeointensity

1 Introduction

The directions of the natural remanent magnetization (NRM) recorded in sedimentary rocks have been used for more than 30 years for the reconstruction of the patterns of polarity reversals and low-frequency secular variations (SV) (as compared with those observed experimentally) of the geomagnetic field (GMF). Although our understanding of the processes by which the sediments acquire their NRM is becoming better and better known, the reliability of depositional and post-depositional remanent magnetizations (DRM and PDRM respectively) as accurate recorders of the field direction is still not accepted by all palaeomagnetists and the possibility of palaeointensity determinations from sediments is more controversial.

2 Depositional and post-depositional magnetization processes

2.1 DRM, PDRM AND DIRECTIONAL VARIATIONS OF THE LOCAL GMF

DRM

DRM results from the physical alignment of individual magnetic grains due to the interaction between their magnetic moments and the ambient magnetic field. The characteristic time of

alignment in water for particles with size from 0.5 to 50 μm varies from 1 to 10 s in fields ranging from 20 to 40 μT (microTesla) (Tucker 1983). The magnetization is locked when the friction due to compaction and viscosity exceeds the magnetic strength. The locking time is controlled by the porosity of the sediment which depends on the rate of deposition and on the grain size of the non-magnetic matrix. Depending on the locking time, the magnetization of sediments can be a DRM (immediate locking) or a PDRM (delayed locking).

PDRM

Under the action of physical disturbance due to external conditions (slumpings, bioturbations, microseisms, movements of gas bubble . . .), the locking is delayed and realignments can occur creating a PDRM.

Irving & Major (1964) experimentally showed the ability of wet artificial sediments containing randomly orientated magnetic particles to acquire a remanent magnetization when subjected to a weak applied field (25–113 μT): the magnetic particles tend to become aligned along the direction of the applied field. Later, Kent (1973) produced PDRMs by stirring and showed that post-detrital realignments of magnetic grains may be induced in natural sediments by physical disturbance such as bioturbation. The intensities of the remanences obtained by Kent were linearly proportional to the strength of the applied field up to 120 μT and good agreement was found between the NRM directions and the applied field direction. The importance of PDRM as an effective process of acquisition of NRM was emphasized by Løvlie (1974, 1976) in his interpretation of his experimental results on the reconstruction of sedimentary records of field reversals. Tucker (1980) showed that PDRM could be produced by slowly stirring a near saturated slurry (*c.* 75 per cent water volume), the PDRM intensity was again found to be linearly proportional to the field.

The limits of the void ratio (water volume/dry sediment volume) allowing the acquisition of PDRM by artificial and natural sediments were defined by Hamano (1980): from 1.4 to 0.9 for the former and from 6 to 3 for the latter types, values which (respectively) correspond to 58–47 and 85–75 per cent of water.

However, some authors still contest the reliability of these processes as recorders of the GMF variations: Biquand (1984) concluded that sediments cannot provide reliable SV records because he found that anomalous directions, diverging from the applied field direction by more than 10° were recorded instantaneously (DRM) by redeposited sediments and he maintained that no post-depositional realignment occurred. Paradoxically, Biquand's results do agree with those of the workers mentioned above as they emphasize the essential effect of post-depositional realignment for accurate recording of the geomagnetic directions.

Although some sedimentary sequences have been shown to yield unreliable results, many more studies have shown that DRM and PDRM acquired in the laboratory under conditions of deposition similar to those occurring naturally and subsequently recovered using suitable laboratory techniques, do yield reliable reconstructions of the geomagnetic field variations they were subjected to.

2.2 DRM, PDRM AND LOCAL GMF INTENSITY VARIATIONS

Since the intensity of the NRM primarily depends on the quality and quantity of magnetic minerals contained in the sediment and secondly on the intensity of the ambient field, the evaluation of the latter requires a normalization of the NRM.

Normalization methods

Levi & Banerjee (1976) suggested that under conditions of magnetic homogeneity along a sedimentary sequence, the anhysteretic remanent magnetization (ARM) could be used to correct the measured NRM for downcore variations in the quantity of remanence bearing grains. The ARM acquired in a 100 μT direct field and a 100 mT (milliTesla) alternating field was chosen as the normalizing parameter because it had the same coercivity spectrum as the NRM as demonstrated by similar alternating field demagnetization curves for both types of magnetizations. They pointed out that their method yielded a SV pattern exhibiting the principal features as obtained from archaeomagnetic results in the interval 400–1800 yr BP. Later, King *et al.* (1982) and King, Banerjee & Marvin (1983) proposed restricted criteria specifying standards of acceptability of the ARM method. However, Tucker (1980, 1981) emphasized the quite different nature of the processes by which NRM and ARM are acquired and argued in favour of methods using stirred remanent magnetization (StRM) as normalization parameter.

An ARM is acquired when an assemblage of magnetic particles is subjected to a decaying alternating magnetic field (af) superimposed on a low direct field (df). It has the same direction than the df and its maximum intensity occurs when the df and the af are parallel. The ARM results from domain wall displacements inside the grains thus, it changes at least partially the initial state of the magnetic domains in the grains, affecting single, pseudo-single and multidomain grains while StRM, resulting from both DRM and PDRM processes, does not change the domain state of the grains, and does not involve the big magnetic grains which are principally subjected to gravitational strengths. Furthermore, the properties of the non-magnetic component of the sediment which interferes with the realignment of magnetic particles during the post-depositional processes are taken in account by the StRM method but totally ignored by the ARM method.

Considering these fundamental differences between the acquisition processes of both types of magnetization, the theoretical superiority of StRM as a normalization parameter is clear in spite of the inappropriate time range of deposition and locking attainable in a laboratory.

In this paper, results of the application of both methods to a 6 m sediment core (B48) from Lac du Bouchet are presented.

3 The late Pleistocene sequence of Lac du Bouchet

3.1 GENERAL COMMENTS

Detailed descriptions of the geological setting of the site, stratigraphy, sedimentology and chronology are given in Bonifay *et al.* (1987) and Creer *et al.* (1986). However, some basic data are presented again here.

The Lac du Bouchet occupies a Maar-type crater located at lat. 44°55′N, long. 3°47′E and altitude 1206 m in the Devès volcanic complex (Haute Loire, France). It is an almost perfect circle of *c.* 800 m diameter and its maximum depth is 27 m. About 40 cores (6, 9 and 12 m long) were collected, mainly from the flat-floored central area using pneumatic Mackereth corers.

3.2 STRATIGRAPHY AND LITHOLOGY

A summary of the lithological succession is as follows:

The upper part (assemblage A) is a brown wet gyttja (80 per cent water content)

containing 20–40 per cent of organic matter. Its thickness varies from 0.5 to 1.5 m (0.85 m in core B48). This level is not completely recovered, especially at the top, due to its high water content. It is underlain by assemblage B which is a dark peat layer 0.10–0.50 m thick (0.48 m in core B48) containing more than 40 per cent of organic matter. The high content of vegetal fibres makes it unsuitable for palaeomagnetic study.

Assemblages A and B correspond to early post-glacial and Holocene conditions. They are characterized by low magnetic susceptibility values due to a low mineral and a high organic content and low sedimentation rates (15 cm kyr^{-1}). Organic contents of less than 10 per cent are typical in the late glacial and glacial sediments. Assemblages C, D and E (1.5–7.5 m depth) consist of clays and silty clays which contain thin sandy layers and turbidites originating from slumpings. These three assemblages are differentiated mainly by their colour. Their organic contents vary from 2 to 10 per cent. The mineral fraction is dominated by fine grains (less than 50 μm in diameter), the coarse grains occurring only in the turbidites and slumps. Assemblage C corresponds to late glacial conditions, D and E to maximum glacial conditions.

High measured sedimentation rates (40–50 cm kyr^{-1}) in assemblages C, D and E indicate active erosion of the crater walls. The magnetic susceptibility 10–15 times greater than in assemblages A and B is attributable to the higher mineral content. Assemblage F found at the base of the longest cores presents an increase both in the water and organic content indicating milder conditions. The climatic conclusions drawn from the lithology, mineralogy and sedimentology were in agreement with those drawn from the pollen analyses by De Beaulieu, Pons & Reille (1984).

In assemblages A and B, the Holocene field record, compressed into about 1–1.5 m of highly organic sediments, does not add anything new to the understanding of the field behaviour in this period. On the contrary, assemblages C, D, E and F give highly stable and

Table 1.

CORE B5	DEPTH (metres)	^{14}C AGE (Yr BP)	SD	DEPTH	POLLEN ZONE (beginning)	AGE
	0.45-0.55	2280	90	0.52	Sub Atlantic	2600
	0.9-0.92	5500	100	0.88	Sub Boreal	4700
				1.3	Atlantic	8000
				1.55	Boreal	9000
	1.6-1.7	8340	150	1.73	Pre Boreal	10300
				1.82	Younger Dryas	10700
				2.00	Bolling/Allerod	13000
	2.8-2.9	15800	900	3.00	Oldest Dryas	15000
	5.3-5.5	19400	1300			
CORE B49 (HEMS)						
	1.75-1.8	9700	200			
	3.00-3.05	12900	180			
	4.20-4.25	14300	250			
	5.00-5.04	19200	300			
	6.00-6.06	23100	600			
	6.61-6.66	27300	900			
	7.10-7.15	28500	900			
	8.12-8.17	30600	1300			

reproducible palaeomagnetic results which provide an entirely new contribution to our knowledge of the late glacial and glacial geomagnetic fields.

3.3 CHRONOLOGICAL DATA AND CORE TO CORE CORRELATIONS

Pollen analyses and radiocarbon dating were carried out on core B5 (5.5 m long) (Bonifay *et al.* 1987). A depth/time transformation curve is proposed in Creer *et al.* (1986). Other radiocarbon datings were done on core B49 (8 m long) using a high energy mass spectrometer (Smith 1985). Table 1 summarizes the whole set of chronological data obtained from Le Bouchet cores B5 and B49. Two transform functions have been computed by Smith for the 0–12 000 yr BP interval and for the 12 000–35 000 yr BP interval, respectively, giving the depth/ime transformation of core B49. Using the characteristic features of the magnetic susceptibility and magnetization intensity, precise correlations were established between each core and core B49. Parameters measured along all the cores could thus be placed on a common chronological scale.

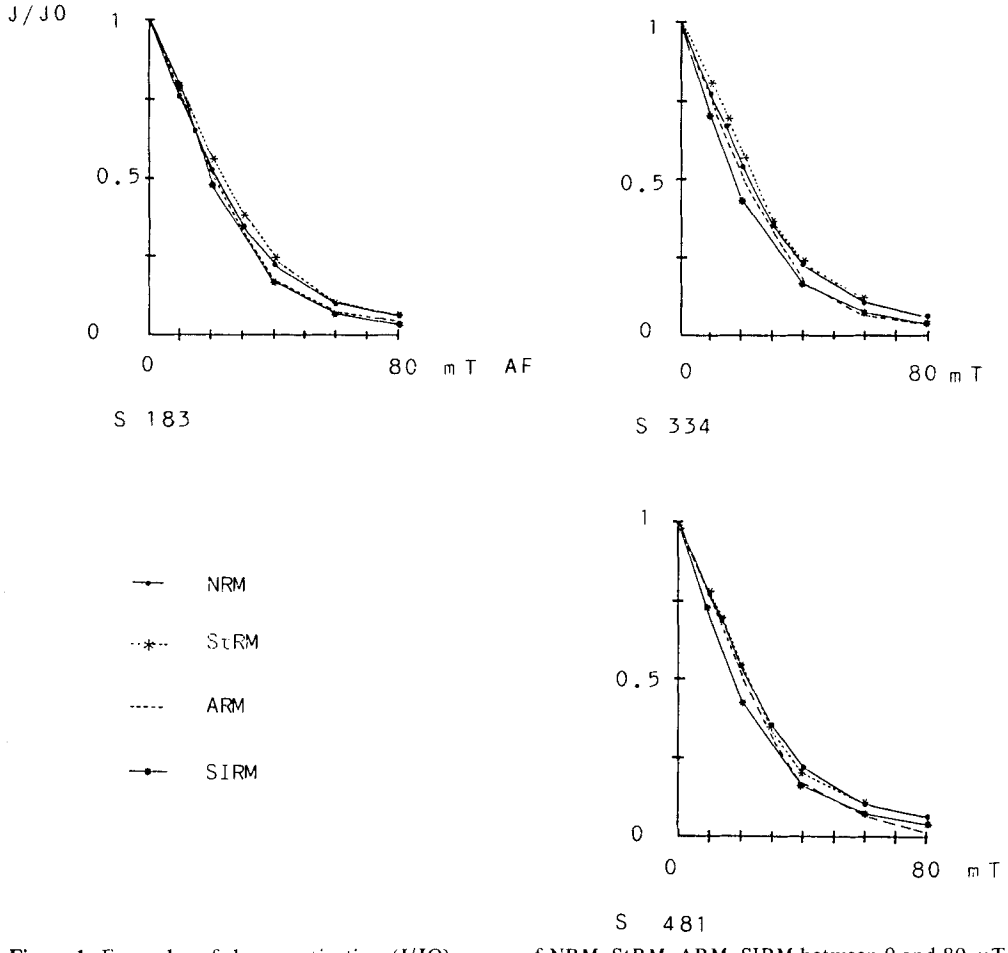

Figure 1. Examples of demagnetization (J/JO) curves of NRM, StRM, ARM, SIRM between 0 and 80 mT showing that the different magnetization have the same range of median destructive field (18–25 mT). Specimens are numbered according to their depth in the core.

4 Palaeomagnetic study of core B48

Palaeomagnetic results previously obtained on about 25 cores spanning from 6 to 12 m depth (20–38 kyr BP) (see Thouveny 1983; Smith 1985; Creer *et al.* 1986; Thouveny & Tucholka 1987) gave directional records which were highly consistent from core to core. These records can be correlated with those of contemporaneous sedimentary sequences studied in other areas (Thouveny *et al.* 1985; Creer 1985) although the Holocene record does not provide highly satisfying results. Some palaeointensity evaluations using the ARM

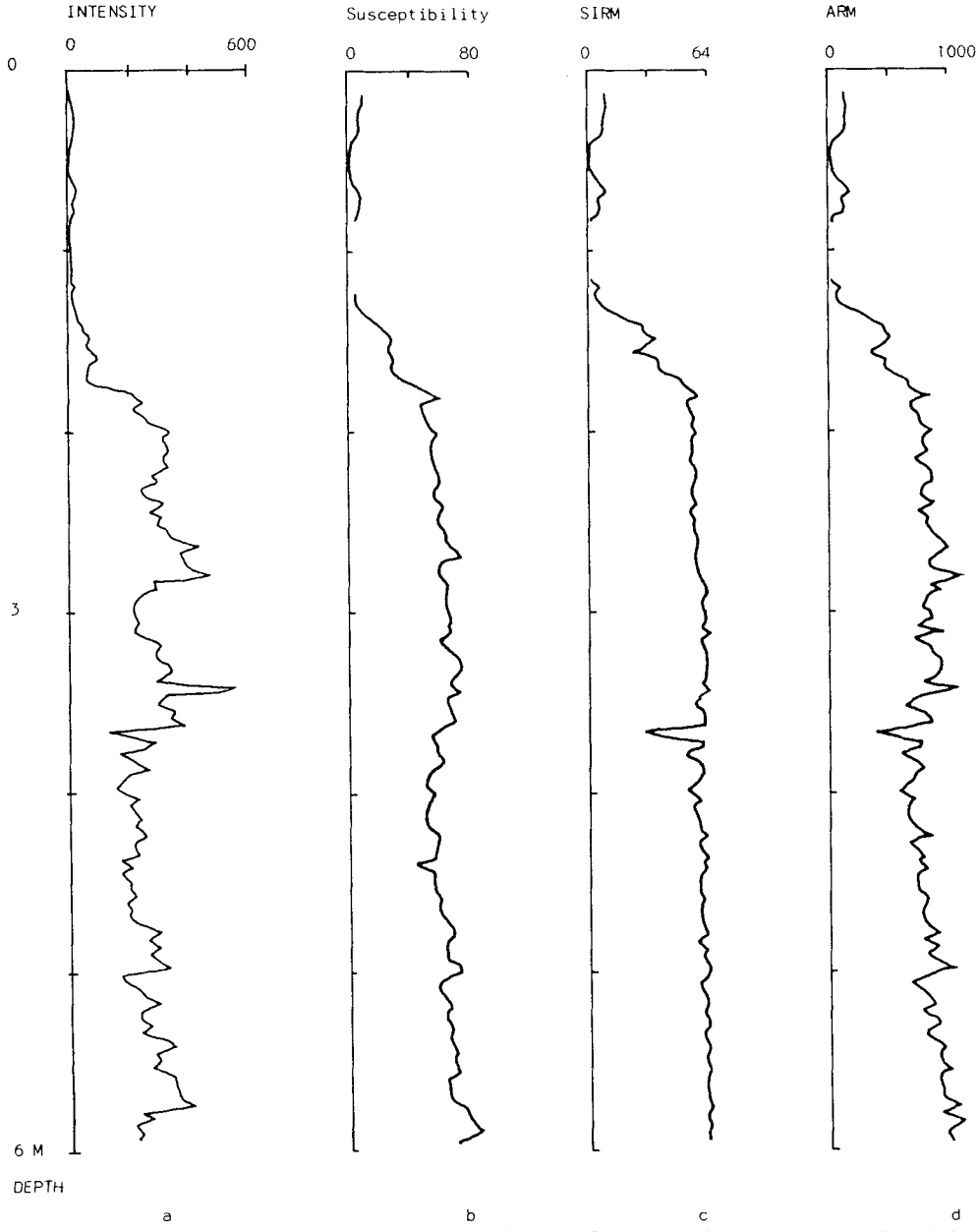

Figure 2. Comparison of the intensity (a), susceptibility (b), SIRM (c), and ARM (d) curves plotted along the depth scale. Respective units are mA m^{-1}, $4\pi \cdot 10^{-6}$ SI, A m^{-1} and mA m^{-1}.

method on these sediments have already been presented and discussed in Thouveny (1983) and Smith (1985).

4.1 SAMPLING

The core (6 m long) was split in two unequal (two-thirds, one-third) parts. Subsampling for the palaeomagnetic analysis and ARM measurements were done by pushing 2 x 2 x 2 cm

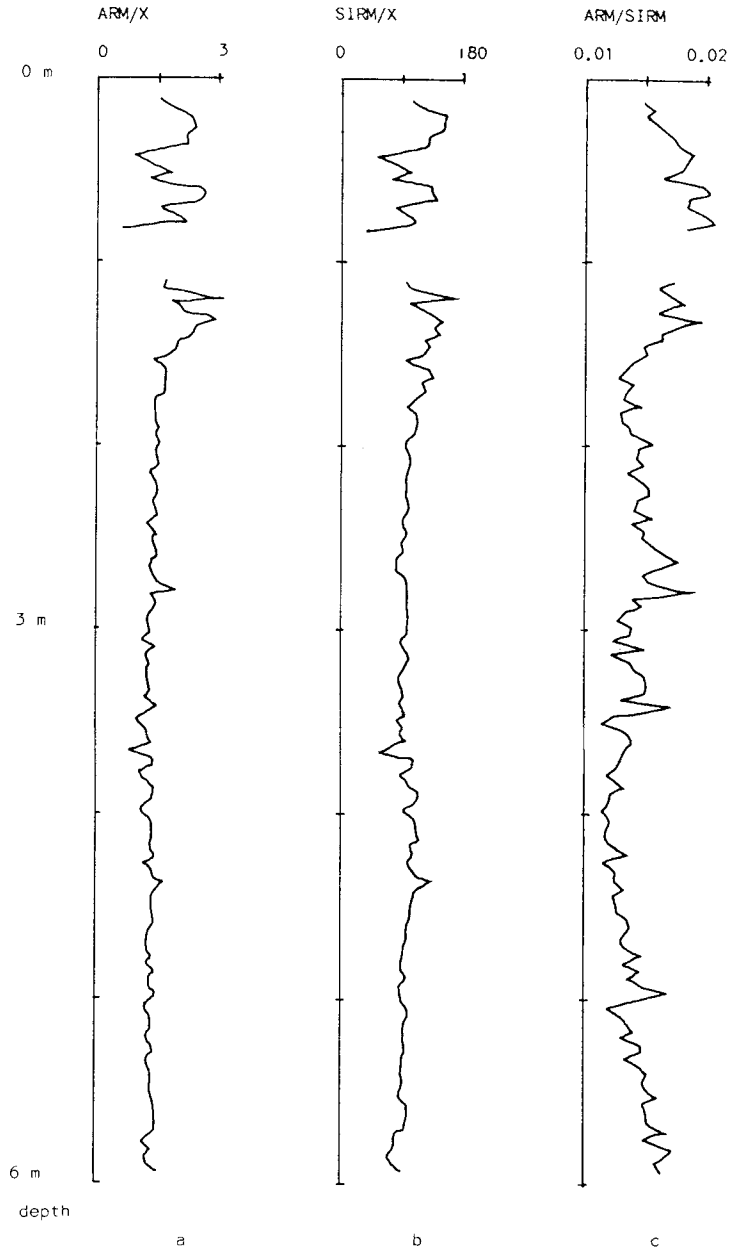

Figure 3. ARM/suscept., SIRM/suscept. and ARM/SIRM ratios expressing the magnetic uniformity along the core. Units are A m^{-1} for (a) and (b) and dimensionless for (c).

plastic boxes into the sediments along the central axis of the two-thirds part at 4 cm spacing (note that the samples are labelled according to their depth in the core). Assemblage B was not subsampled. The sediment remaining (70 cm^3) was collected in plastic bags.

4.2 MEASUREMENTS

All the remanence measurements were done using a Digico spinner magnetometer connected to a microcomputer. Alternating field (af) demagnetizations were carried out with a Schonstedt GSD1 demagnetizer. The susceptibilities were measured on the individual specimens after drying, in order to normalize the susceptibility to the weight of dry sediment.

The NRM was measured on the whole set of specimens. Ten pilot specimens were then demagnetized stepwise in peak fields from 5 to 80 mT. The orthogonal projection diagrams attest to a high directional stability after the initial removal (10 mT) of a weak viscous component. The intensity curves reveal median destructive field (MDF) values ranging from 20 to 30 mT (Fig. 1). A bulk demagnetization at 10 mT was then applied to all specimens in order to remove the viscous magnetization.

The amplitude of the oscillations is $\pm 50^\circ$ for declination and $\pm 25^\circ$ for inclination around the mean direction ($D = 0^\circ$; $I = 65^\circ$ for the NRM and $D = 0^\circ$; $I = 66^\circ$ for the 10 mT cleaned directions) which may be compared with the field direction at the site due to the geocentric axial dipole ($D = 0^\circ$; $I = 63.4^\circ$). The inclination variation recorded in the glacial and late glacial sequence is presented in Fig. 7(a) as a function of the time.

Susceptibility and intensity (Fig. 2a, b) show an abrupt change at 1.75 m and several minor oscillations below 1.75 m. The most pronounced susceptibility and intensity peaks were used for the correlation between cores B48 and B49. The intensity curve shows large amplitude oscillations superimposed on the magnetic content variations which could be due to the recording of medium- to long period palaeointensity changes. This represents an encouraging preliminary observation for NRM normalizations.

5 ARM normalization method

5.1 CONDITIONS OF VALIDATION

King *et al.* (1982, 1983) argued that ARM intensities can be reliably used to estimate the variations in the concentration of magnetic minerals carrying the NRM, provided the carriers are magnetite grains in the size range 1–15 μm [usually termed pseudo-single domain (psd) to fine multidomain (md) grains]. Magnetic grains smaller than 1 μm contribute a disproportionately high ARM compared with DRM and PDRM, whereas those larger than about 15 μm may exhibit true multidomain behaviour and consequently yield a viscous or unstable NRM. Thus, large variations of the grain size will affect the NRM/ARM ratio. Furthermore, the concentration along the core should vary by a factor of less than 20–30 times the minimum.

For determining the average grain size of magnetite, Banerjee, King & Marvin (1981) and King *et al.* (1982, 1983) compared the initial susceptibility to the anhysteretic susceptibility (defined as the ARM acquired in a 10 mT af and a 0.1 mT df) of samples in which the size of the grains was controlled. Since ARM principally affects small grains and susceptibility considers also the big grains, the ARM/suscept. ratio varies like the reverse function of the grain size: from 2.5 $A\,m^{-1}$ for 1 μm diameter to 0.5 $A\,m^{-1}$ for 20 μm diameter.

Saturation isothermal remanent magnetization (SIRM) is also principally carried by small grains. The SIRM/suscept. ratio also varies as a reverse function of the grain size: 5×10^4 $A\,m^{-1}$ for monodomain (< 1 μm) and 10 to 10^3 $A\,m^{-1}$ for psd or fine md particles.

However, as the superparamagnetic grains (size < 0.05 μm for magnetite) will be considered in the susceptibility measurements, the ARM/SIRM ratio is then preferably used.

Hilton (1986) theoretically demonstrated and experimentally verified that normalized magnetic parameters (ARM/suscept., SIRM/suscept., ARM/SIRM) can be independent of the magnetic mineral concentration only if (i) a single mineral is present in the sample, (ii) the relative concentration of each magnetic mineral to the others remains constant or (iii) only one mineral on a constant background of other minerals changes in concentration. In the general case (number of magnetic minerals unknown), mineralogy and domain size are not likely to be deduced.

The normalized parameters cited here can still give ideas on the variation of concentrations along the sedimentary column.

5.2 MAGNETIC MINERALOGY AND CONCENTRATION IN THE LAC DU BOUCHET SEDIMENTS

The criteria recommended by King *et al.* were tested by Smith (1985) on the Lac du Bouchet cores by the following experiments:

(i) Hysteresis loops: 95 per cent of the saturation isothermal magnetization (SIRM) was obtained before 250 mT. The S100 ratio (back IRM at 100 mT/back SIRM) varies from 150 to 220 along the core. The small range of the coercive forces defined along the core (36.7–40 mT) shows a relative uniformity of the grain size.

(ii) Curie temperature determined on magnetic extracts ranged between 520 and 560°C (Curie temperature of pure magnetite is 575°C).

These two tests demonstrate that the main magnetic carrier is magnetite possibly with a small titanium content.

(iii) X-ray fluorescence analyses of a magnetic extract showed that iron and titanium were contained in 1.5 and 5 μm grains.

(iv) In spite of Hilton's conclusions, values of SIRM/suscept. (50–500 A m^{-1}) are still consistent with the dominance of psd or md magnetite. The relatively small variations of the SIRM/suscept., ARM/suscept., and ARM/SIRM ratios indicated a reasonable stability of the magnetic concentration along the core.

The susceptibility, NRM, ARM and SIRM curves confirm that the concentration of magnetic minerals is much lower in the Holocene sediments (0–2 m depth) than in the Pleistocene sediments (2–12 m depth).

In this study, the consistency of the magnetic mineralogy of core B48 with the other cores has been tested here by susceptibility, IRM growth and bulk measurements of ARM and SIRM (Fig. 2c, d). As justified in the next section, the bulk ARM was produced by the application of a 80 mT alternating field together with a 35 μT direct field. While this does not exactly reproduce the 'anhysteretic susceptibility' recommended by King *et al.* (1982) (100 mT af and 100 μT df), the stable value of the ARM/X ratio (*c.* 1.5 A m^{-1}) again lies in the range suggested for psd to fine md magnetite of *c.* 5 μm diameter (Fig. 3a). The SIRM was produced by a 0.25 T direct field which is quite sufficient to ensure saturation. The value of the SIRM/X ratio oscillates around 100 A m^{-1} (Fig. 3b). The predominance of psd to fine md magnetite as the main magnetic carrier is thus confirmed. The general stability of the ARM/X, SIRM/X and ARM/SIRM ratios along the 1.7–6.0 m section certifies the quantitative uniformity of the magnetic content (Fig. 3a, b, c).

The good agreement between the determinations of grain sizes and domain states given by the different methods suggests that we could deal with one of the three particular cases proposed by Hilton.

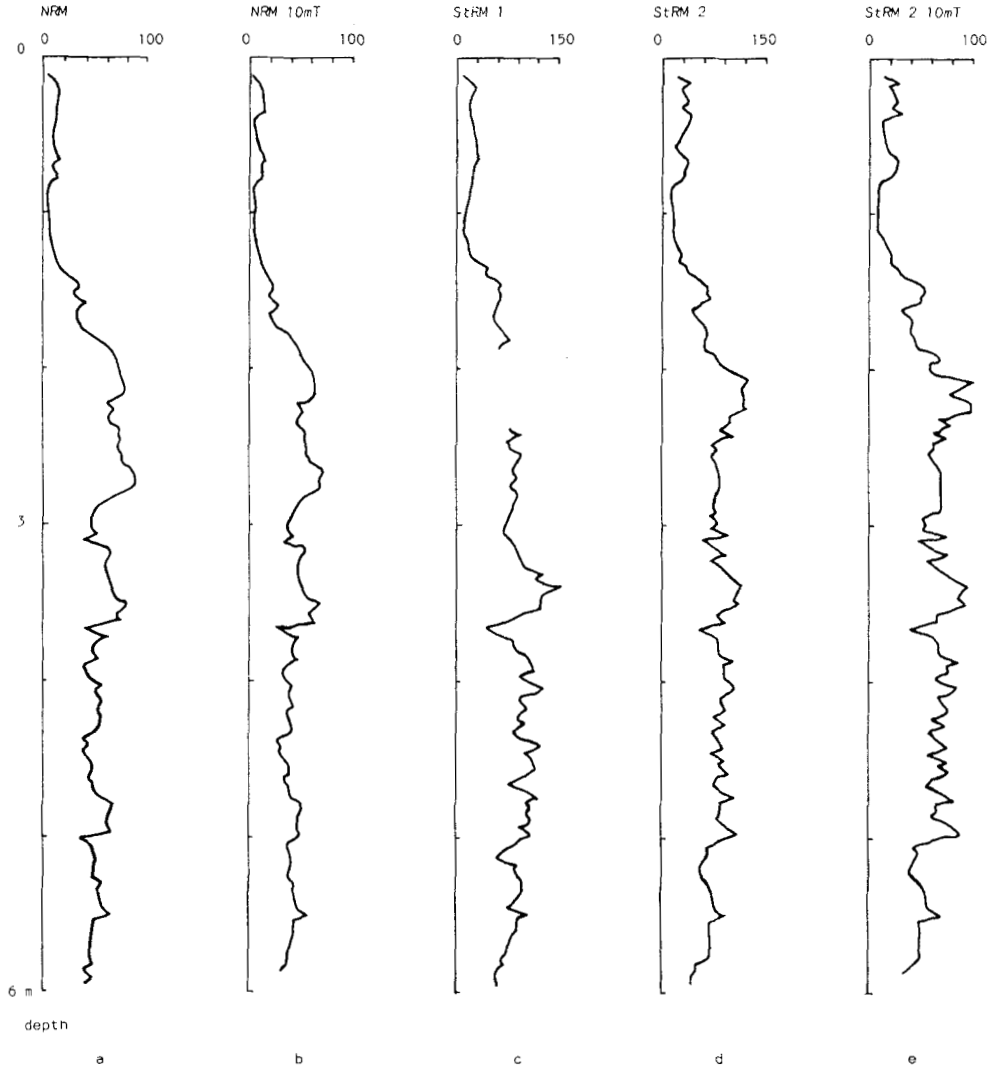

Figure 4. Comparison of the specific (weight normalized) NRM (a), NRM 10 mT demagnetized (b), StRM first (c) and second generation (d, e). Units are in A m^{-1} kg^{-1}.

5.3 CHOICE OF THE ARM PARAMETERS

Ten pilot specimens were subjected to the combined effects of stepwise increasing alternating fields (20–80 mT) and a weak direct field parallel to the alternating field (horizontal component of the laboratory field = 35 μT). The ARMs obtained were stepwise AF demagnetized from 0 to 80 mT. The 20, 40 and 60 mT af combined with the direct field produce magnetizations having much weaker resistance to af demagnetization than the NRM, the MDFs range from 5 to 15 mT. The ARM produced by the combination of the 35 μT df and a 80 mT af has the same resistance to af demagnetization as the NRM until the MDF is reached (MDF of both types of magnetization lie in the same range) (Fig. 1). In higher demagnetizing fields, the ARM remaining is softer than the NRM. One can notice that the SIRM is carried by lower coercivity particles than the ARM: its demagnetization curve lies below the ARM demagnetization curve. The ARM given by a 80 mT alternating

field and a 35 μT direct field has been retained as the best approximation of the NRM obtainable by this method under these experimental conditions: each specimen has been subjected to this treatment, measured and demagnetized in 10 mT af.

5.4 CURVE ANALYSIS

An obvious similarity appears between the Q ratio, NRM/SIRM and NRM/ARM curves (Fig. 6a, b, c) but the latter presents smoother trends than the former two. The smoothing is improved by the use of the NRM10/ARM10 ratio (Fig. 6d). As already emphasized, the results obtained above and below 1.75 m depth must be considered separately: above 1.75 m, the ratio varies from 0.1 to 0.25; below 1.75 m, the mean value of the ratio as well as the amplitude of the variations are increased (0.25 to 0.65). Between 1.8 and 6 m, one major oscillation is observed on which three or four minor oscillations are superposed.

6 Redeposition and stirred remanent magnetization (StRM)

6.1 PREVIOUS WORK

Tucker (1980) has shown theoretically and experimentally that the main parameters controlling the proportionality of the intensity of the stirred remanent magnetization versus the applied field are the stirring rate and the water content. Low stirring rates (*c.* 1 Hz) applied to near saturated slurries (*c.* 75 per cent of water) in the presence of a geophysically realistic magnetic field result in the acquisition of a PDRM called stirred remanent magnetization (StRM) which is proportional to the field and reproducible with less than ±15 per cent error. The acquisition is completed after few tens of seconds following the end of the disturbance. The experimental results follow the theoretical model satisfactorily.

The following equation is assumed to be valid:

$$NRM/StRM = k \cdot Hp/Hex.,$$

where Hp is the palaeofield strength and Hex the experimental field strength. The value of k depends essentially on the discrepancies between the natural and experimental processes of acquisition of the remanence: for example, time and compaction do not interfere in experimental conditions. Furthermore, the proportion of the viscous remanent magnetization (VRM) remaining after 10 mT cleaning, in the NRM can not be precisely evaluated. The NRM/StRM ratio must then be considered as a reliable but relative evaluation of the Hp/Hex ratio, even if both magnetizations are previously cleaned.

6.2 METHOD

A wood surface of 1 m^2 was isolated from magnetic and metallic influences. The laboratory field strength was equal to 50 μT with an inclination of 58°. Its stability in space and time was controlled before starting the redeposition. The field strength was observed to vary by no more than ±1 per cent over the surface and the temporal variations recorded during 10 hr were of similar magnitude. The first generation of redeposition experiments was separately carried out on three successive subsets of samples from the upper half of the core (intervals 0–1.8, 1.8–2.8 and 2.8–3.8 m) using the smallest (most homogeneous) experimental area. However, for the lower part of the core as well as for the second generation experiments, the possibility of higher amplitude temporal variations was considered and only two subsets of samples were treated separately: 0–5 and 3–6 m.

6.3 FIRST GENERATION StRM

About 130 samples (70 cm^3) of wet sediment were mixed by hand with additional water in order to obtain a homogeneous saturated slurry (more than 80 per cent of water). The slurries were poured into rectangular plastic boxes (5.5 x 4.2 x 3.8 cm inner dimensions). The boxes were carefully placed on the horizontal wood surface, with their long axis parallel to the horizontal component of the laboratory field. Stirring was performed in each sample independently with a glass rod at a rate of about 2 spins s^{-1} for 10–12 s. The excess water was siphoned off after 10–20 hr. The sampling was carried out after four days using the standard boxes (as used for the NRM).

The remaining sediment was kept wet in each box for the second generation deposit. Measurements of the StRM and stepwise af demagnetization of pilot specimens were immediately carried out. After measurement, all the specimens were dried in 58°C and weighed: the specific (weight normalized) StRM could be compared with the specific NRM, the variation of the NRM/StRM ratio is then free of the differential water content errors.

6.4 SECOND GENERATION OF StRM

The same samples (wet sediment remaining in the boxes) were mixed again with water until a near saturated slurry (*c.* 70 per cent of water) was obtained.

The same stirring procedure as for the first generation was employed. The sampling was carried out after drying for four days in the applied field. Two specimens of each slurry sample were taken so that the internal consistency of the intensity results could be tested: the specific intensity of each specimen was compared with that of its twin and the maximum acceptable variation was set to 10 per cent. The NRM/StRM ratio curve was produced using the mean StRM value of the twin samples.

The StRM were then af demagnetized in a 10 mT field in order to remove any spurious magnetization acquired during the subsampling process or just before measurements and principally, to normalize the 10 mT cleaned NRM.

The variations of the first and second generation specific (weight normalized) StRMs are plotted in Fig. 4(c, d, e).

Three criteria were used for the elimination of spurious specimens:

(1) Heterogeneity or discontinuity of the sedimentary structures noticed either in the natural sediment or in the redeposited sediment or disturbance during handling.

(2) The magnetic susceptibility (X) was measured on the dried individual specimens and normalized on the dry weight. The ratio $Xi = X \cdot g^{-1}_{NRM}/X \cdot g^{-1}_{StRM}$ measured along the core, indicates eventual changes in the magnetic concentration between the original (NRM) and reconstituted (StRM) samples. The mean value of Xi equals 0.96 which does not differ significantly from the theoretical value (=1), with a standard deviation = 0.11.

The samples whose ratio Xi was different from $Xi \pm$ s.d. were considered as non-representative of the level and the results from them were rejected.

(3) The individual directions of the StRM are plotted in Fig. 5. When deviations of more than 15° from the field direction are recorded, the alignment was considered as spurious.

The value of the NRM/StRM ratios were rejected if any one of these criteria was not satisfied. Only five samples were rejected in the 1.75–6.00 m interval.

7 Analysis of the results

The stability of the StRM was tested by a stepwise af demagnetization performed on pilot specimens. The J/JO curves are closely similar to those of the NRM and the median

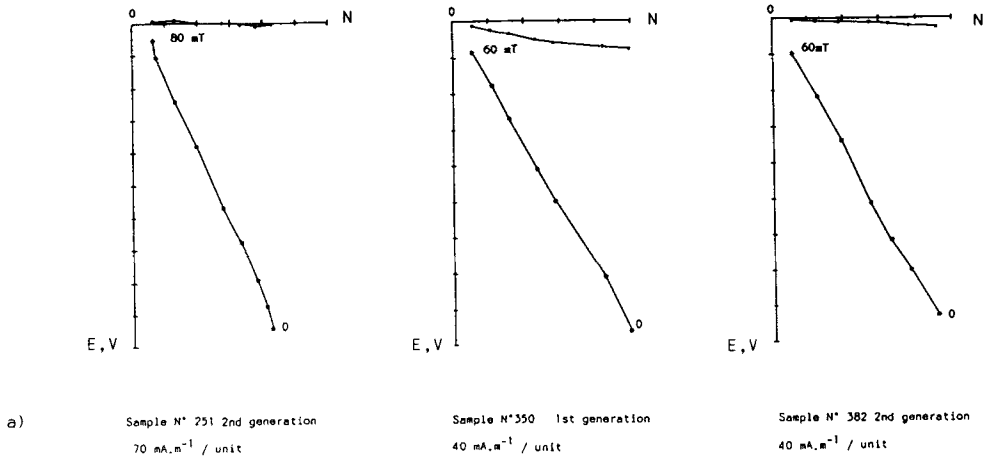

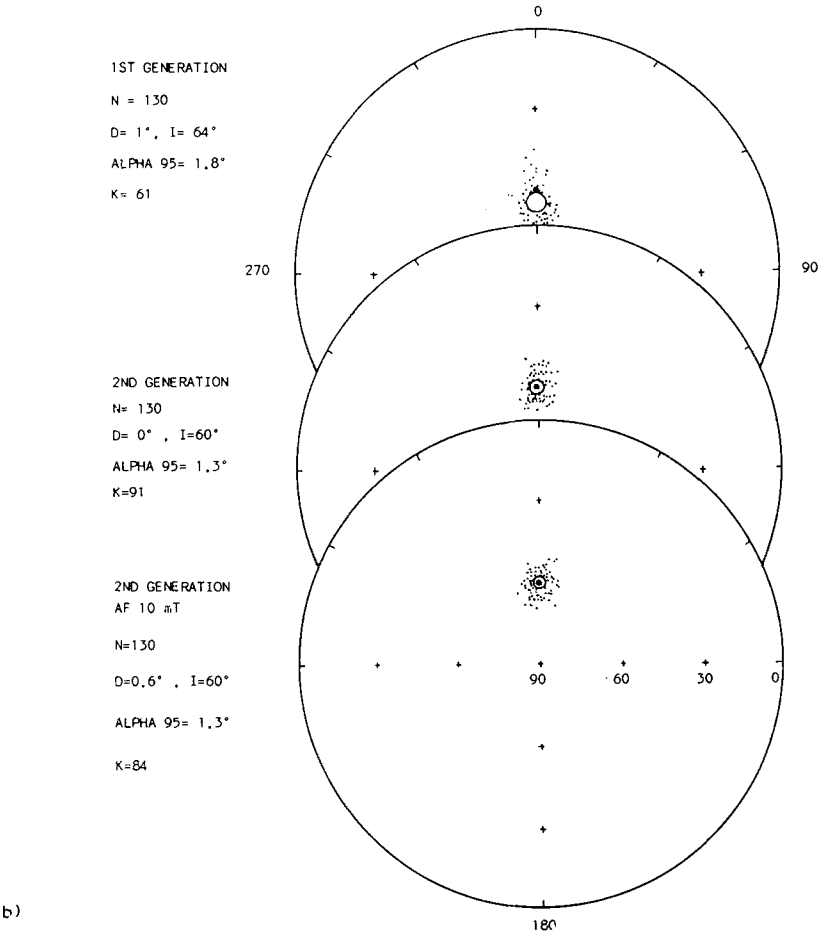

Figure 5. (a) Orthogonal projection diagrams of the alternating field demagnetization (0–80 mT) of StRM first and second generations specimens. N, north; E, east; V, vertical. (b) Stereographic projections of the individual directions of the StRMs. Circles represent the highest density area of the points distribution. Stars figure the direction of the dipole field at the site. Alpha 95 could not be drawn on the figures but Fisher statistical parameters and mean directions are given.

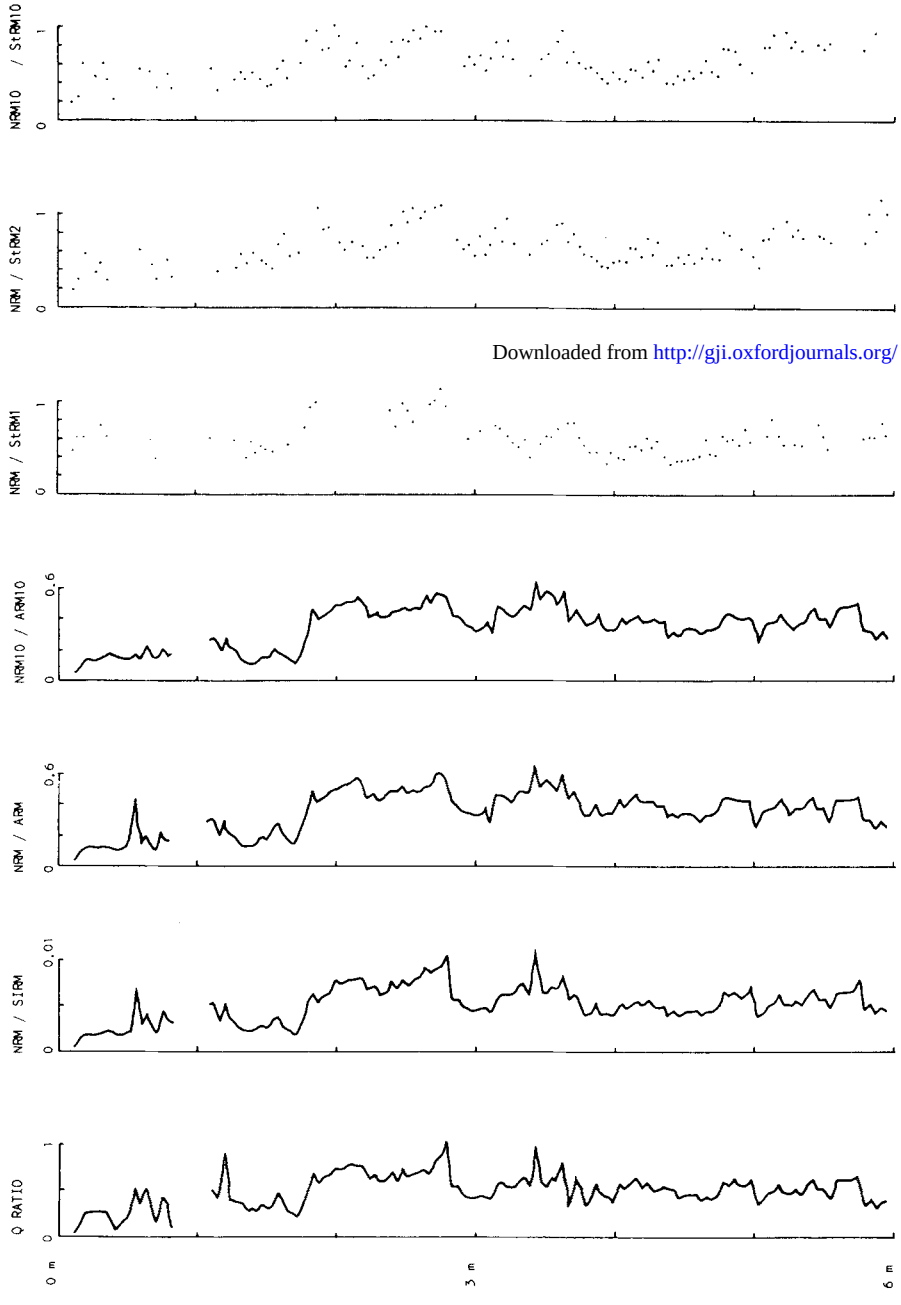

Figure 6. Comparison of the normalization processes of the NRM: Q ratio (a), NRM/SIRM (b), NRM/ARM (c), NRM10/ARM10 (d), NRM/StRM (e), NRM/StRM2 (f) and NRM 10 mT/StRM 10 mT (g). Units are mA m^{-1} (a) and dimensionless (b, c, d, e, f, g).

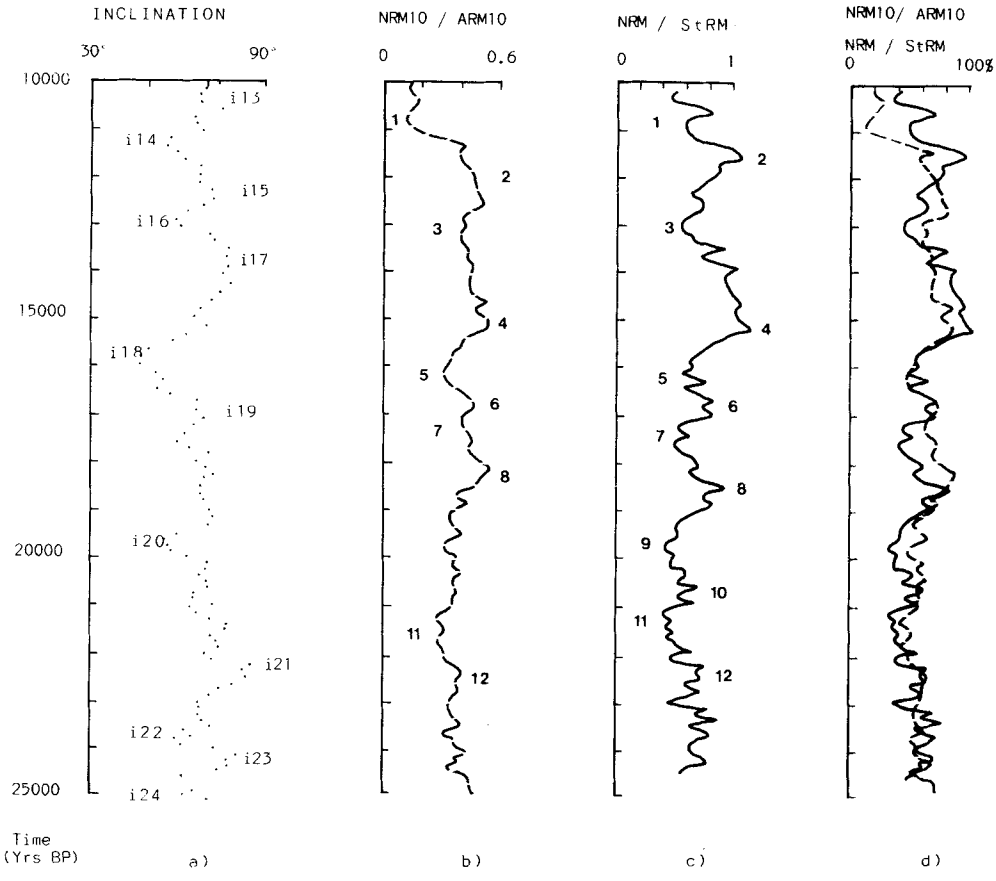

Figure 7. Inclination (a), NRM10/ARM10 (b), NRM/StRM (c). (d) presents (b) and (c) plotted together on a 100 per cent horizontal scale. All the parameters are plotted on a time-scale of 10 000–25 000 yr BP. Inclination and relative palaeointensity peaks are (respectively) labelled i13 to i24 and 1 to 12. The NRM/StRM curve (c) is drawn from arithmetical averaging at each level of the NRM/StRM1 and NRM/StRM2 values presented in Fig. 6(e) and (f).

destructive fields (MDFs) lie in the same range (20–25 mT) (Fig. 1). The orthogonal projection diagrams show a high directional stability (Fig. 5a).

7.1 StRM DIRECTIONS (FIG. 5b)

For the first generation of experiments, the mean inclination (64°) is 6° higher than the laboratory field inclination; the mean declination (0.9°) is not significantly different from the North. For the second generation, the mean inclination (59.8°) is only 2° higher than the lab field inclination, the mean declination (0.2°) is very satisfactory. The statistical parameters show that the first generation directions present a greater dispersion than the second generation directions. This can be attributed to the fact that the first generation slurries were more than 10 per cent richer in water than the second generation: the effects of stirring may have been less effective than in the former case. Thus, the lower water content of the second generation slurries might have resulted in a RM acquisition process which corresponds closer to the natural PDRM acquisition process than that of the first generation.

7.2 NRM/StRM RATIO CURVES

Comparison of the first and second generation curves (Fig. 6e, f) shows that both the general shapes and the scatter of the values are similar except for the 1.8–2.8 m interval for which the first generation results are scattered while the second generation results yield a well-defined feature. The first generation results obtained in this interval were rejected because they showed surprisingly high StRM intensities and StRM/X ratios, such that it is inferred that a rapid and important increase of the ambient field strength must have occurred during the drying process though no directional inconsistency could be noticed. It is stressed that the same methodology was employed along the whole core and that the X_{NRM}/X_{StRM} ratios were close to unity. Comparing the two successive intervals 1.8–2.8 and 2.8–3.8 m (noted 1 and 2), their mean NRM and susceptibility were found to be similar; their respective mean StRM intensities would then be assumed to be similar too. The effect of the field strength change could then be corrected by multiplying the individual StRM of the interval 1 by a correction factor taken as the ratio of the respective mean StRM: $StRM_2/StRM_1$.

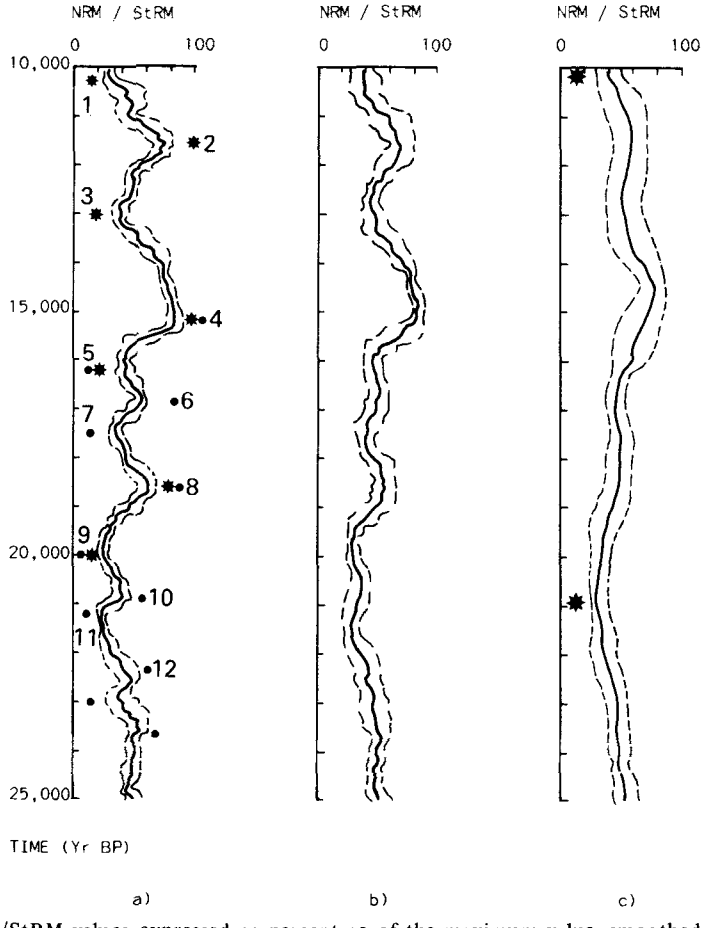

Figure 8. NRM/StRM values expressed as percentage of the maximum value, smoothed by the running mean method: (a) window 500 yr, step 100 yr; (b) window 1000 yr, step 100 yr; (c) window 2000 yr, step 200 yr. The main periods are defined by symbols: ✱11 000 yr, * 3000–3500 yr and • 1500–2000 yr. Broken line give the confidence interval at each level.

However, the scatter recorded in the StRM values of the interval 1 indicates that the sharp increase of the field strength had not the same effect on each individual sample of this interval. These samples were then definitely rejected from the first generation results.

The second generation StRM were demagnetized at 10 mT, the NRM10/StRM10 ratio, plotted in Fig. 6(g) alongside the first and second generation results, shows that no significant improvement in the scatter of the data results from this treatment. A mean curve was drawn from the arithmetic average of the first and second generation NRM/StRM at each level. The transformation on the chronological scale (B49) is allowed by the precise correlation of the susceptibility profiles between cores B48 and B49. The variation of the principal parameters studied here (inclination, NRM/ARM and NRM/StRM) can then be expressed as a function of time (yr BP) (Fig. 7).

8 Discussion of the results

A great number of data obtained from the Holocene period had to be rejected, the data plotted in this interval still show a great dispersion. As already observed on the lithology and magnetic mineral content, the climatic change between post-glacial and Holocene periods induced sedimentological variations which are not compatible with the use of the NRM/ARM method for normalization purposes. It also seems that both sedimentation rates and magnetic mineral content in the Holocene levels are not really suitable for normalization purposes with the StRM method.

On the contrary, the 10 000–25 000 yr interval gives well-clustered data which define regular oscillations on both NRM/ARM and NRM/StRM profiles. However, it is noticeable that the sharp maxima or minima of the ARM/X, SIRM/X, ARM/SIRM ratio indicating abrupt changes in the grain size or concentration of the magnetic particles correspond to sharp maxima and minima of the NRM10/ARM10, the individual specimens carrying these values were simply rejected from the construction of the NRM10/ARM10 curve presented in Fig. 7(b); no other smoothing or filtering procedure was employed.

A relatively satisfying correspondence between the relative palaeointensity results obtained by both methods (ARM and StRM) can be deduced from the first observation of Fig. 7(b, c, d). Maxima and minima occur approximately at the same time in both profiles although a phase shift can sometimes appear (peak 8) but peak amplitudes are obviously different. For example, the amplitude of peaks 1 and 2 is much higher in the first case (Fig. 7b); this trend can be correlated with the big change in the magnetic mineral content at the end of the late glacial and shows that the NRM/ARM normalization method is far from being perfectly efficient in this interval, although the magnetic uniformity was indicated by the appropriate parameters. On the contrary, oscillations 2, 3, 4 have a much lower amplitude in the first case (Fig. 7b) than in the second case (Fig. 7c). This discrepancy was already noticeable on the ARM and StRM curves (Figs 2d, 4c, d, e) and could be inferred to the differences of acquisition processes stated in Section 2.2.

Further interpretations and discussions will preferably consider the palaeointensity evaluations provided by the StRM normalization method in the interval 10 000–25 000 yr BP.

9 Interpretation

9.1 PERIODS AND AMPLITUDES OF THE OSCILLATIONS

Considering the lowest and highest values of the palaeointensity on the whole interval, it can be noted that the former (peaks 1 and 11) occur (respectively) at about 10 000

and 21 000 yr BP and the latter (peak 4) occur at 15 000 yr BP. A long period oscillation (T = 10 000–11 000 yr) with a peak to peak amplitude about 60 per cent of the maximum value can then be defined which is better shown up by further smoothing (1000 and 2000 yr window shifted with a 100 and 200 yr step) (Fig. 8b, c).

- Three shorter period oscillations (*c.* 3500 yr) are easily recognizable (peaks 1, 2, 3; 3, 4, 5 and 5, 6, 7), their peak to peak amplitude lie from 40 to 50 per cent of the maximum value.
- Minor trends are superimposed with periods of 1500–2000 yr and peak to peak amplitudes of 20–30 per cent of the maximum value.

Further precision in the periodicities requires a detailed spectral analysis which could not be performed in this work. However, the main and most obvious periodicities observed here (11 000, 3500 and 1500–2000 yr) lie in the same range as those (11 050, 3800, 2100 and 1365 yr) defined on the inclination oscillations recorded in the same time interval for the same site, by the maximum entropy method and the Fourier transform method (Smith 1985; Smith & Creer 1986).

9.2 COMPARISON WITH FORMER RESULTS

As the data obtained from the Holocene cannot be considered; few former palaeointensity results are available for a comparison in the studied time interval. However, some indications can be drawn from the comparison with the geomagnetic dipole moment (GDM) curve proposed by McElhinny & Senanayake (1982).

(1) A significant increase in the GDM moment appears between 20 000 and 25 000 yr and 10 000 and 15 000 yr, which is consistent with the curve proposed here and points out the possibility of longer period oscillations.

(2) The 11 000 yr period recognized here, extrapolated towards present times leads to a broad maximum of the field strength at about 4000 yr BP which could correspond to the maximum of the GDM indicated around 2500–3000 yr BP by the archaeomagnetic data.

10 Conclusion

The stirred remanent magnetizations obtained on two generations of redeposited and stirred sediments are shown as having the same stability against magnetic cleaning as the NRM. They give reliable records of the direction of the experimental field. Taken as a normalization parameter of the NRM, the repeated StRMs yield highly comparable profiles of the relative palaeointensities along the lower 4 m of the core.

Furthermore, in spite of some discrepancies the mean NRM/StRM profile shows a reasonable correspondence with the NRM/ARM profile obtained on the same core: minimum and maximum peaks of both curves generally occur at the same levels (same time) also roughly corresponding to minimum and maximum peaks of the inclination. After transformation to a time scale, the principal periods could be estimated. In the 10 000–25 000 yr interval, a major period of 11 000 yr could be defined which might be assigned to the variation of the dipole field. The most obvious period lies around 3500 yr although shorter period oscillations (1500–2000 yr) are superimposed. This range of periodicities can be compared to those (T = 2400 yr and T = 2750 yr) respectively suggested by the historically recorded rate of westward drift and by the comparison of the European and North American palaeosecular variation type curves on the interval 0–10 000 yr (Creer & Tucholka 1983b). These periodicities may then be inferred to the drift of the non-dipole foci.

A broad maximum of the geomagnetic field strength occurred 15 000 yr BP and broad minimum values occurred at 21 000 and 10 000 yr BP.

Acknowledgments

I am particularly grateful to Professor K. M. Creer for his advice and critical reading of the manuscript and to Dr G. Turner who helped to clarify many points by providing a highly detailed refereeing report, including correction of grammatical errors.

References

Banerjee, S. K., King, J. & Marvin, J., 1981. A rapid method for magnetic granulometry with applications to environmental studies, *Geophys. Res. Lett.*, **8**, 333–336.

Beaulieu, J. L., De, Pons, A. & Reille, M., 1984. Recherches pollenanalytiques sur l'histoire de la végétation des Monts du Velay, Massif Central, France, *Diss. Bot.*, **72**, 45–70.

Biquand, D., 1984. Mise en evidence d'une erreur de fossilisation du champ magnétique terrestre dans un depot actuel, *Can. J. Earth Sci.*, **21**, 1325–1334.

Bonifay, E., Creer, K. M., De Beaulieu, J. L., Casta, L., Delibrias, G., Perinet, G., Pons, A., Reille, M., Servant, S., Smith, G., Thouveny, N., Truze, E. & Tucholka, P. (1987). A study of the Holocene and late Wurmian sediments of Lac du Bouchet (Haute Loire, France): first results, in *Climate: History, Periodicity and Predictability*, ed. Rampino, M. R. *et al.*, Van Nostrand Rheinhold, Stroudsbourg, Penn.

Creer, K. M., 1985. Review of lake sediments Palaeomagnetic data, *Geophys. Surv.*, **7**, 125–160.

Creer, K. M. & Tucholka, P., 1983a. Epilogue, in *Geomagnetism of Baked Clays and Recent Sediments*, pp. 273–305, eds, Creer, K. M., Tucholka, P. & Barton, L., Elsevier, Amsterdam.

Creer, K. M. & Tucholka, P., 1983b. On the current state of lake sediments palaeomagnetic research, *Geophys. J. R. astr. Soc.*, **74**, 223–238.

Creer, K. M., Smith, G., Tucholka, P., Bonifay, E., Thouveny, N. & Truze, E., 1986. A preliminary palaeomagnetic study of the Holocene and late Würmian sediments of Lac du Bouchet (Hte Loire, France), *Geophys. J. R. astr. Soc.*, **86**, 943–964.

Hamano, Y., 1980. An experiment on the post-depositional remanent magnetization in artificial and natural sediments, *Earth planet. Sci. Lett.*, **51**, 221–232.

Hilton, J., 1986. Normalized magnetic parameters and their applicability to palaeomagnetism and environmental magnetism, *Geology*, **14**, 887–889.

Irving, E. & Major, A., 1964. Post-depositional detrital remanent magnetization in a synthetic sediment, *Sedimentology*, **3**, 135–143.

Kent, D. V., 1973. Post-depositional remanent magnetization in Deep Sea sediments, *Nature*, **246**, 32–33.

King, J. W., Banerjee, S. K., Marvin, J. & Ozdemir, O., 1982. A comparison of different magnetic methods for determining the relative grain size of magnetite in natural materials: some results of lake sediments, *Earth planet. Sci. Lett.*, **59**, 404–419.

King, J. W., Banerjee, S. K. & Marvin, J., 1983. A new rock magnetic approach to selecting sediments for geomagnetic palaeointensity studies: application to palaeointensity for the last 4000 yrs, *J. geophys. Res.*, **88**, 5911–5921.

Levi, S. & Banerjee, S. K., 1976. On the possibility of obtaining palaeointensities from lake sediments, *Earth planet. Sci. Lett.*, **29**, 219–226.

Løvlie, R., 1974. Post-depositional remanent magnetization in a redeposited Deep-Sea sediment, *Earth planet. Sci. Lett.*, **21**, 315–320.

Løvlie, R., 1976. The intensity pattern of post-depositional remanence acquired in some marine sediments deposited during a reversal of the external magnetic field, *Earth planet. Sci. Lett.*, **30**, 209–214.

McElhinny, M. W. & Senanayake, W. E., 1982. Variations in the geomagnetic dipole 1: the past 50 000 yrs. *J. geomagn. Geoelect., Kyoto*, **34**, 39.

Smith, G., 1985. Late glacial palaeomagnetic secular variations from France, *PhD thesis*, University of Edinburgh.

Smith, G. & Creer, K. M., 1986. Analysis of geomagnetic secular variations 10 000 to 30 000 years BP, Lac du Bouchet, France, *Phys. Earth planet. Int.*, **44**, 1–14.

Thouveny, N., 1983. Etude paléomagnétique de formations du Plio-Pleistocène et de l'Holocène du

Massif central et de ses abords: contribution à la chronologie du Quaternaire, *Thèse de 3è cycle*, Université d'Aix-Marseille II.

Thouveny, N. & Tucholka, P., 1987. Marqueurs géomagnétiques fins dans le Pleistocène, in *Geologie des Lacs et Paleolacs*, Traveaux du CERLAT, Vol. 1, Le Puy en Velay, in press.

Thouveny, N., Creer, K. M., Smith, G. & Tucholka, P., 1985. Geomagnetic oscillations and excursions and upper Pleistocene chronology, *Episodes*, **8**, 180–182.

Tucker, P., 1980. Stirred remanent magnetization: a laboratory analogue of post-depositional remanent magnetization, *J. Geophys.*, **48**, 153–157.

Tucker, P., 1981. Palaeointensities from sediments: normalization by laboratory redeposition, *Earth planet. Sci. Lett.*, **56**, 398–404.

Tucker, P., 1983. Magnetization of unconsolidated sediments and theory of DRM, in *Geomagnetism of Baked Clays and Recent Sediments*, pp. 9–19, eds Creer, K. M., Tucholka, P. & Barton, Elsevier, Amsterdam.